J. Fluid Mech. (1967), *vol.* 30, *part* 1, *pp.* 51–64
Printed in Great Britain

Theoretical and experimental investigations of the reflexion of normal shock waves with vibrational relaxation

By N. H. JOHANNESEN, G. A. BIRD† AND H. K. ZIENKIEWICZ
Department of the Mechanics of Fluids, University of Manchester

(Received 7 February 1967)

The one-dimensional problem of shock-wave reflexion with relaxation is treated numerically by combining the shock-wave, characteristic, and Rayleigh-line equations. The theoretical results are compared with pressure and density measurements in CO_2, and the agreement is found to be excellent.

1. Introduction

The majority of experimental determinations of vibrational relaxation times have been based on shock-tube studies of the relaxation region behind shock waves travelling into the gas at room temperature. The relaxation process is described by the simple equation

$$\frac{d\sigma}{dt} = \rho\Phi(\bar{\sigma} - \sigma), \tag{1}$$

where σ is the vibrational energy and $\bar{\sigma}$ its equilibrium value, ρ the density, and $\Phi = \Phi(T)$, the relaxation frequency, which is assumed to be a function of the translational temperature, T, only. Most experimenters have evaluated Φ for the relaxation region as a whole and then ascribed it to some mean value of the temperature within the relaxation region. More detailed evaluations (Johannesen, Zienkiewicz, Blythe & Gerrard 1962; Zienkiewicz & Johannesen 1963) show that Φ is not strictly a function of T only. This effect is small, however, and can be neglected in most engineering applications.

It has tacitly been assumed by most investigators that the values of Φ determined from shock-wave experiments on gases at room temperature before the shock could be used for the calculation of other types of flow pattern, in particular the reverse process of expansion, either steady or unsteady.

Recent experiments by Hurle, Russo & Hall (1964) threw serious doubt on this assumption. They found values of Φ more than an order of magnitude higher in expanding nozzle flows than in shock waves. This result has since been confirmed by several investigators but questioned by others. An up-to-date survey will be published in the *Proceedings* of the 7th AGARD Colloquium on Recent Advances in Aerothermochemistry held at Oslo in May 1966. There is obviously

† On sabbatical leave from Department of Aeronautical Engineering, University of Sydney.

an urgent need for more experimental work on different flows with relaxation to try to clarify the situation, and the present investigation was stimulated by this need. As it happens, the work did not throw much light on the actual values of the relaxation frequency but it does show up a number of features of considerable interest.

The flow to be investigated must satisfy two requirements: it must lend itself to accurate experimentation as well as to accurate theoretical calculations. This, of course, severely limits the possibilities. The reflexion of a shock wave from the end wall of a constant-area tube has been investigated extensively by a number of workers. It is well known that the interaction between the reflected wave and the boundary layer is very severe, in particular for gases with low specific heat ratio such as CO_2. Photographs showing such interactions have been taken in this department and published by Dyner (1966). It is obvious that the flow has been modified by the shock-wave boundary-layer interaction to an extent that makes any comparison with a one-dimensional theory very crude indeed.

There is, however, a region in time and space for which the flow is truly one-dimensional. Immediately after the reflexion, disturbances originating at the corners travel towards the centre-line of the tube both along the reflected shock wave and in the region behind it. Until these disturbances, which are clearly visible in the monochromatic interferogram in figure 1, plate 1, reach the centre-line, the flow there is truly one-dimensional. This means that pressure records at the centre of the wall will correspond to one-dimensional flow for a certain time interval after the reflexion.

An interferometer record will never be truly one-dimensional because it displays the integrated effects across the whole of the working section and disturbances similar to those shown on figure 1, plate 1, will be present near the glass windows. On figure 1 the disturbances are expansion waves originating at a narrow gap between the end wall and the roof and floor of the tube. However, in our particular shock tube the working section is 2 in. $\times$ 8 in. with the longer dimension in the direction of the light path and the distortion of the record is sufficiently small to be either negligible or to amount to only a small correction.

It is therefore reasonable to assume that sufficiently accurate experimental results can be obtained. The theoretical calculations must be based on a characteristic network step-by-step procedure combined with the shock-wave and Rayleigh-line equations. Using the heat-transfer analogy (Johannesen 1961) in which the flow is treated as that of an ideal gas (the α-gas) with heat extraction equal to the transfer of energy into the vibrational mode, the formulation of the problem and the calculation procedure is straightforward in principle.

It turns out that to obtain sufficient accuracy the number of steps involved and the number of machine instructions (of the order 10^8) are so large that the calculations can only be carried out in a reasonable time by the fastest computers available. In our case the Manchester University Atlas computer was used.

The calculations were first carried out for a general gas with vibrational relaxation and the general features of the flow are discussed in some detail.

Then calculations were made for specific flows in CO_2 and comparisons made with pressure records obtained by Baganoff at GALCIT and with our own inter-

ferometer records of density distributions. In both cases the agreement between theory and experiment is remarkably good.

The work does not throw much additional light on the controversy about the numerical values of the relaxation frequency. In fact, it is found that, for CO_2, values of the relaxation frequency obtained from single shock waves do not only give an adequate description of the reflected shock-wave problem in their own temperature range but can be used when extrapolated to much higher temperatures than those obtained in single shock waves.

2. Flow of a universal gas

To investigate the general properties of the flow it is convenient to operate with what might be called a universal diatomic gas with vibration, but without dissociation. Phinney (1964) has shown that the available experimental results on the relaxation frequency for diatomic gases (with the exception of the recent nozzle data) collapse to a good degree of accuracy into a universal curve if Φ/Φ_θ, the ratio of the relaxation frequency to its value at the characteristic temperature of vibration, is plotted against T/θ.

The first set of calculations were made for this universal gas using the harmonic oscillator expression for the vibrational energy.

It is convenient to introduce non-dimensional variables. θ is the obvious choice of a characteristic temperature. A characteristic velocity is then $(R\theta)^{\frac{1}{2}}$, where R is the gas constant. The scale of the relaxation region in any flow will depend on Φ, which can be non-dimensionalized with respect to Φ_θ, and on the pressure, which can be non-dimensionalized with respect to a reference pressure. In the present case a natural choice is p_1, the pressure ahead of the incoming shock. The non-dimensional ('hatted') variables are then defined by the following equations:

$$\left.\begin{matrix} u \\ a \end{matrix}\right\} = (R\theta)^{\frac{1}{2}} \left\{\begin{matrix} \hat{u}, \\ \hat{a}, \end{matrix}\right. \quad (2)$$

$$T = \theta\hat{T}, \quad (3)$$

$$p = p_1\hat{p}, \quad (4)$$

$$\rho = \frac{p_1}{R\theta}\hat{\rho}, \quad (5)$$

$$s = R\hat{s}, \quad (6)$$

$$c_{v\alpha} = R\hat{c}_{v\alpha}, \quad (7)$$

$$\Phi = \Phi_\theta\hat{\Phi}, \quad (8)$$

$$\sigma = R\theta\hat{\sigma}, \quad (9)$$

$$x = \frac{[R\theta]^{\frac{1}{2}}}{p_1\Phi_\theta}\hat{x}, \quad (10)$$

$$t = \frac{R\theta}{p_1\Phi_\theta}\hat{t}. \quad (11)$$

Here u is the particle velocity relative to the wall, a the frozen speed of sound, s the specific entropy of the α-gas, $c_{v\alpha}$ the specific heat at constant volume of the α-gas, and x and t the space and time co-ordinates, respectively.

The characteristic equations for one-dimensional unsteady flow at constant area with heat transfer are given by Shapiro (1954, p. 976). His heat transfer term q is in our case equal to $-D\sigma/Dt$ and the equations become

$$\frac{d\hat{x}}{d\hat{t}} = \hat{u} \pm \hat{a}, \quad (12)$$

$$\frac{d\hat{p}}{\hat{\rho}} \pm \hat{a}\,d\hat{u} = -(\gamma_\alpha - 1)\frac{D\hat{\sigma}}{D\hat{t}}\,d\hat{t}, \quad (13)$$

$$\frac{D\hat{\sigma}}{D\hat{t}} = \hat{\rho}\hat{\Phi}\,(\bar{\hat{\sigma}} - \hat{\sigma}), \tag{14}$$

$$\hat{p} = \hat{\rho}^{\gamma_\alpha}(\text{const}) \exp \frac{\hat{s} - \hat{s}_1}{\hat{c}_{v\alpha}}, \tag{15}$$

$$d\hat{s} = \frac{-d\hat{\sigma}}{\hat{T}}. \tag{16}$$

Phinney's expression for the relaxation time becomes in our notation

$$\hat{\Phi} = \hat{T} \exp[-7{\cdot}394(\hat{T}^{-\frac{1}{3}} - 1)]. \tag{17}$$

The harmonic oscillator expression for the vibrational energy is

$$\hat{\sigma} = [\exp(\hat{T}^{-1}) - 1]^{-1}. \tag{18}$$

These equations are used to calculate the flow in region 3 (figure 2) behind the reflected shock wave. They must be matched to the standard shock-wave equations for the reflected shock wave and these themselves must be matched to the Rayleigh-line equations (Johannesen 1961) which describe the relaxation region behind the incoming shock. This region travels at constant speed equal to that of the incoming shock and conditions are therefore given at any point in region 2 in the (x, t)-diagram between the incoming and reflected shock waves.

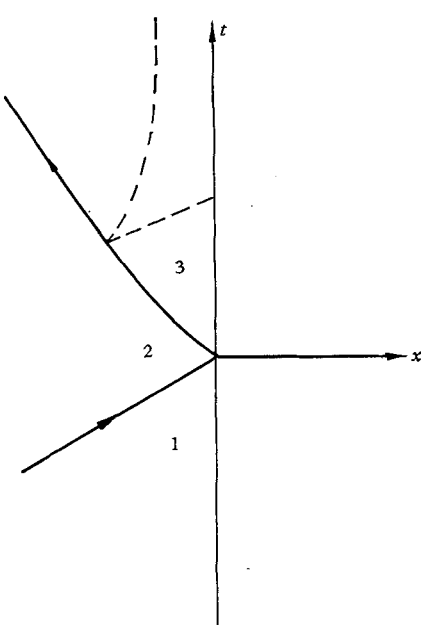

FIGURE 2. (x, t)-diagram.

The network in region 3 is based on the particle paths and one family of ordinary characteristics (the family with $dx/dt = 1/(u+a)$). For each new point in the network interpolation is carried out along the backward characteristic of

the other family. This particular choice of network combines the advantages of the Eulerian and Lagrangian formulations of the equations of motion. One remains in the (x,t)-diagram and therefore retains the advantages of easy physical interpretation. At the same time the calculations follow the behaviour of individual particles of fluid, an obvious advantage in the case of non-isentropic flow.

A typical program was based on 100 network points along the reflected shock wave. The running time on the Atlas computer was 7 min. This type of calculation gave sufficient accuracy near the point of reflexion but did not quite reach large enough values of x and t for equilibrium to have been established. The program output was given in the form of tables of $\hat{x}, \hat{t}, \hat{u}, \hat{p}, \hat{T}, \bar{\hat{\sigma}}$ and $\hat{\sigma}$ at the network points. The density can be found directly from the equation of state, which with our non-dimensional variables takes the simple form

$$\hat{p} = \hat{\rho}\,\hat{T}. \tag{19}$$

The output data can be plotted in two ways. The variation of the various quantities with time at the end wall ($\hat{x} = 0$) can be plotted directly (figure 3). By interpolation values for a fixed value of $\hat{t}$ can be plotted as functions of $\hat{x}$,

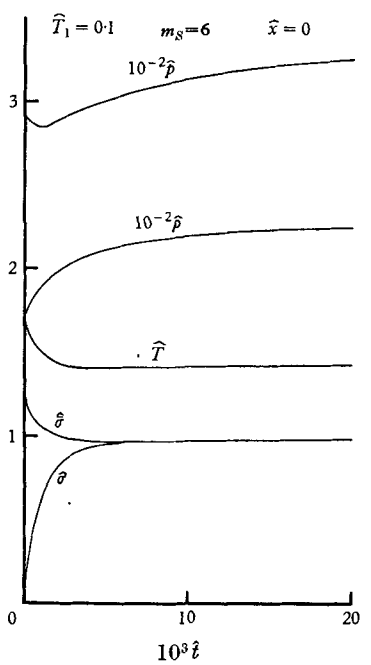

FIGURE 3. Variations with $\hat{t}$ at $\hat{x} = 0$ for reflected shock wave in a universal diatomic gas with $\hat{T}_1 = 0{\cdot}1$ and $m_S = 6$.

giving the variation through a slug of gas as on figure 4. This interpolation was carried out on a desk machine, as it would have been very lengthy to program and taxed the memory of Atlas beyond its capacity.

We shall now discuss the two representations in detail with reference to figures 3 and 4 for a temperature in front of the incoming shock $\hat{T}_1 = 0{\cdot}1$ and frozen shock Mach number $m_S = 6$. (We use m and M to indicate Mach numbers based on frozen and equilibrium sound speeds, respectively.)

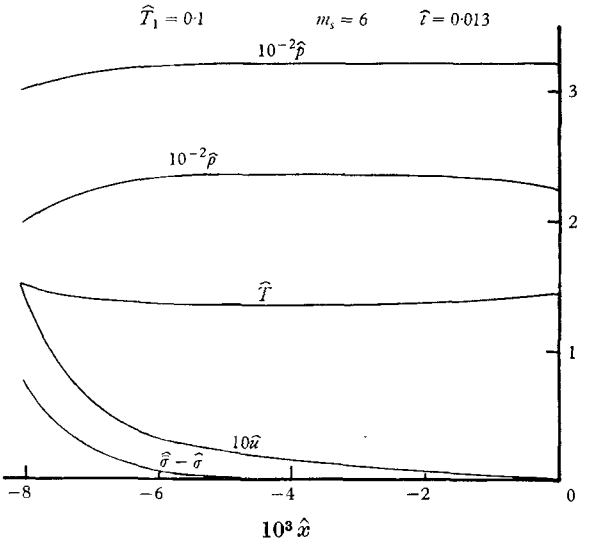

FIGURE 4. Variations with $\hat{x}$ at $\hat{t} = 0{\cdot}013$ for reflected shock wave in a universal diatomic gas with $\hat{T}_1 = 0{\cdot}1$ and $m_S = 6$.

On the end wall the temperature starts off at its frozen/frozen value, falls rapidly to a minimum and then increases very gradually to its equilibrium value. Equilibrium has not quite been reached on the figure. The equilibrium value of the vibrational energy does of course show the same behaviour as the temperature. The actual energy in vibration starts off at the negligibly small value ahead of the incoming shock and then rapidly increases to the local equilibrium value. We notice that the time required for $(\bar{\hat{\sigma}} - \hat{\sigma})$ to become negligibly small is much smaller than the time required to reach final equilibrium. There are therefore two time scales involved in the relaxation process behind the reflected wave.

The density increases monotonically from its frozen/frozen value to final equilibrium. However, the pressure behaves in a rather unexpected manner. $\hat{p}$ falls rapidly to a minimum value, which occurs much earlier than the minimum in $\hat{T}$, and then increases monotonically to its equilibrium value. This behaviour of $\hat{p}$ was predicted by Baganoff (1965), who argued that under certain conditions the pressure corresponding to frozen transition through the incoming shock followed by very rapid adjustment behind the reflected shock was lower than both the frozen/frozen and equilibrium/equilibrium values. We shall return to this question in some detail later.

Detailed inspection of our results confirms Baganoff's finding that the time required for the pressure to reach equilibrium on the wall is governed by the relaxation time behind the incoming shock. He also noted that the pressure variation at the wall is quite large so that the pressure is a convenient quantity

to use for experimental observations. This is in contrast with the situation behind the incoming shock, where the pressure variation through the relaxation region is quite small. A comparison between experiment and theory for the pressure on the wall is given in § 3.

Turning now to figure 4, we first note that this corresponds to a time two-thirds of full scale on figure 3. This means that all properties at the wall are close to their final equilibrium values and the situation is very similar to that at a very large time where one would expect a stationary entropy layer close to the wall and a relaxation region behind the reflected wave travelling with the speed of the wave and leaving a steadily growing intermediate region with constant properties.

We note that the particle velocity $\hat{u}$ is everywhere directed towards the wall. The entropy layer at the wall leads to an increase in $\hat{T}$ and a marked decrease in $\hat{\rho}$. Behind the reflected wave the variables behave as in the usual relaxation region behind a shock wave travelling into a uniform region.

On figure 4 the density curve lends itself to direct experimental observation by means of interferometry and a comparison between theory and experiment is given in § 4.

3. Comparison between theoretical and experimental pressure distributions

The work described so far was carried out independently of the work by Baganoff now to be discussed. Contact was established with Baganoff, who has designed a fast-response pressure gauge (Baganoff 1964) and published a number of pressure records (Baganoff 1965). The latter paper also contains a detailed discussion of the expected shape of the pressure curve. He failed to observe the dip in the pressure curve experimentally and therefore concluded that his theoretical argument suggesting such a dip was incorrect.

The computation method outlined above for a universal diatomic gas with vibrational relaxation can easily be adapted to cope with a specific gas, diatomic or polyatomic. For carbon dioxide we select as reference temperature, θ, the characteristic temperature of the bending mode, $\theta_2 = 959\,^\circ\mathrm{K}$. The harmonic oscillator expression for the vibrational energy then becomes

$$\frac{\overline{\sigma}}{R\theta_2} = 2\left[\exp\left(\frac{\theta_2}{T}\right)-1\right]^{-1} + \frac{\theta_1}{\theta_2}\left[\exp\left(\frac{\theta_1}{T}\right)-1\right]^{-1} + \frac{\theta_3}{\theta_2}\left[\exp\left(\frac{\theta_3}{T}\right)-1\right]^{-1}, \quad (20)$$

where $\theta_1 = 1920\,^\circ\mathrm{K}$ and $\theta_3 = 3380\,^\circ\mathrm{K}$. This expression was considered sufficiently accurate for our present purpose as it only differs from the values tabulated by Hilsenrath *et al.* (1955) by about 3 % at the maximum temperature ($\sim 5000\,^\circ\mathrm{K}$) in the experiment.

The Φ values were obtained from the values given on figure 5 in the paper by Johannesen *et al.* (1962). First a mean point was chosen for each value of M_1 and these points were then fitted by a smooth curve. The expression is

$$\hat{\Phi} = \hat{T}\exp\left[2{\cdot}02 - 2{\cdot}48\hat{T}^{-\frac{1}{3}}\right]\left[1-\exp\left(-\hat{T}^{-1}\right)\right]^{-1}. \quad (21)$$

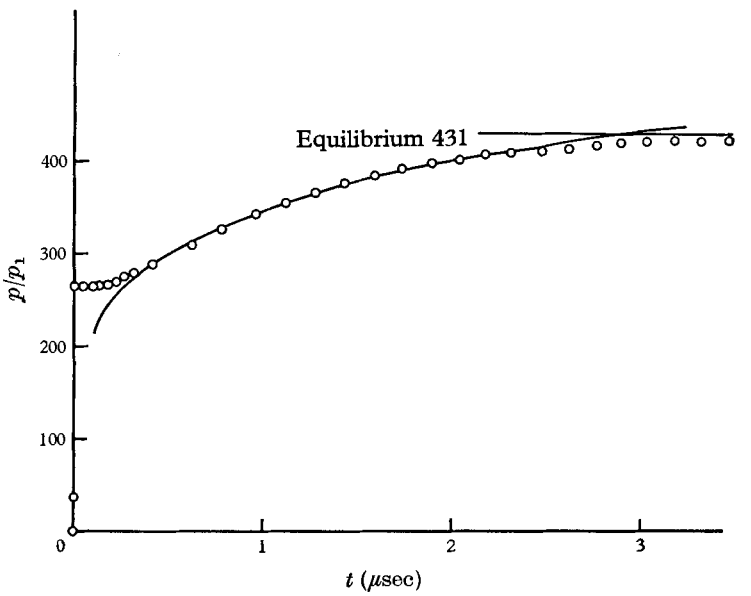

FIGURE 5. Wall-pressure variation for reflected shock wave in CO_2 with $T_1 = 300$ °K, $p_1 = 1$ mmHg and $M_S = 5{\cdot}98$ (large time scale). O, large steps. Baganoff run no. 648.

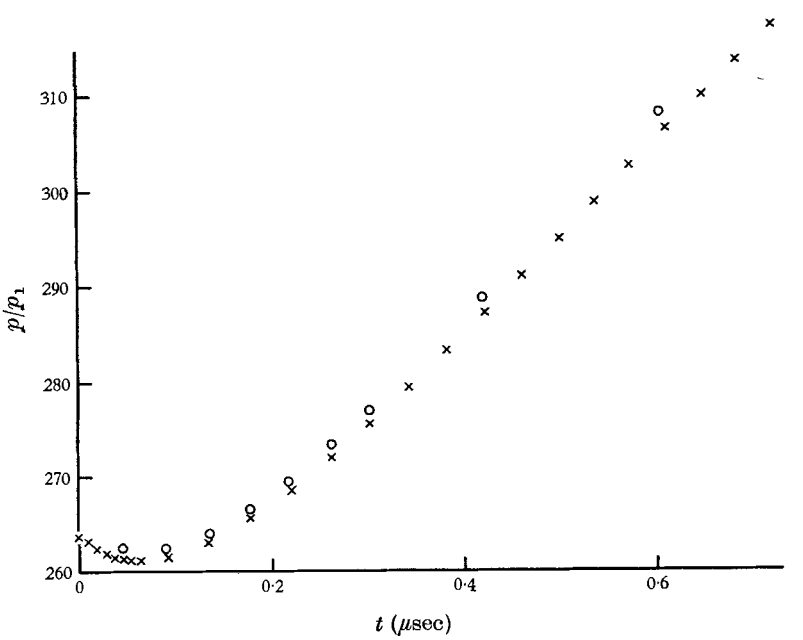

FIGURE 6. Wall-pressure variation for reflected shock wave in CO_2 with $T_1 = 300$ °K, $p_1 = 1$ mmHg and $M_S = 5{\cdot}98$ (small time scale). ×, small steps; O, large steps.

This is only a curve-fit and no physical meaning should be given to the last term. This numerical expression was used through the whole temperature range, a very considerable extrapolation.

Figure 5 shows a comparison between the theoretical and experimental pressure curve for a shock wave of $M_S = 5{\cdot}98$ in CO_2 at initial pressure 1 mmHg.† The general agreement is remarkable. The theoretical results are shown as the actual calculated points. There is an indication of a very slight dip in the pressure curve. To investigate the region immediately after the reflexion in more detail the computation was repeated with a five times smaller step size and the results are shown together with those with larger steps on figure 6. The effect of step size on the accuracy is clearly demonstrated; it amounts to about 1 % in p for the larger values of t. There is now no doubt about the presence of a minimum in the pressure curve but it is very shallow and occurs at less than $0{\cdot}1\,\mu$sec after the reflexion, so it is not surprising that it was not detected on the pressure record in figure 5.

In view of Baganoff's statement that his experimental results contradict his theoretical conclusion that there should be a dip in the pressure curve, an analytical expression was obtained for $(\partial p/\partial t)_{t=0}$, the initial pressure gradient at the wall. The derivation is given in the appendix and leads to

$$\left(\frac{\partial \hat{p}}{\partial \hat{t}}\right)_{t=0} = \frac{\hat{\Phi}_2(\hat{\bar{\sigma}}_2 - \hat{\bar{\sigma}}_1)}{\hat{c}_{p\alpha}\hat{T}_1^2} G(m_2)\left[F(m_2) - \frac{\Gamma_3}{\Gamma_2}\right], \tag{22}$$

where

$$\Gamma = \phi(\bar{\sigma} - \sigma) \tag{23}$$

and G and F are universal functions of m_2, the α-gas Mach number behind the incoming shock wave relative to the wave.

It is found that for the particular expression used for CO_2 the pressure gradient is negative if $M_S > 2$ and positive if $M_S < 2$ for a shock travelling into CO_2 at 295 °K.

It is worth noting that for lower Mach numbers it might be possible to obtain pressure records showing the dip.

4. Comparison between experimental and theoretical density distributions

The instantaneous density distribution between the wall and the reflected shock wave was found for a number of shocks in CO_2, using the interferometer technique described by Johannesen *et al.* (1962) and making due allowance for dispersion (Zienkiewicz, Johannesen & Gerrard 1963). The white light interferograms had central fringe patterns similar to the monochromatic pattern shown in figure 1, plate 1. The fringe shift measured was between region 2 and region 3 (figure 2) and the absolute density in region 3 was found by assuming the density in region 2 to be the equilibrium density behind a shock travelling at the measured Mach number of the incident shock. Figures 7 and 8 show typical results and the agreement between theory and experiment is again remarkably good.

† We are grateful to Dr Baganoff for supplying the oscilloscope record.

For $M_S = 1{\cdot}51$ (figure 7) the experimental density curve is about 1 % below the theoretical one. An estimate of the effect of the density reduction due to the expansion waves from the corner between the end wall of the shock tube and the glass windows showed this to be of order 1 %, giving complete agreement with theory. This is considered to be fortuitous, as the overall accuracy of the measurements can hardly be claimed to be better than 1 %.

On figure 8 ($M_S = 3{\cdot}97$) two additional effects are apparent. There is a slight distortion of the density curve in the region behind the reflected wave due to the

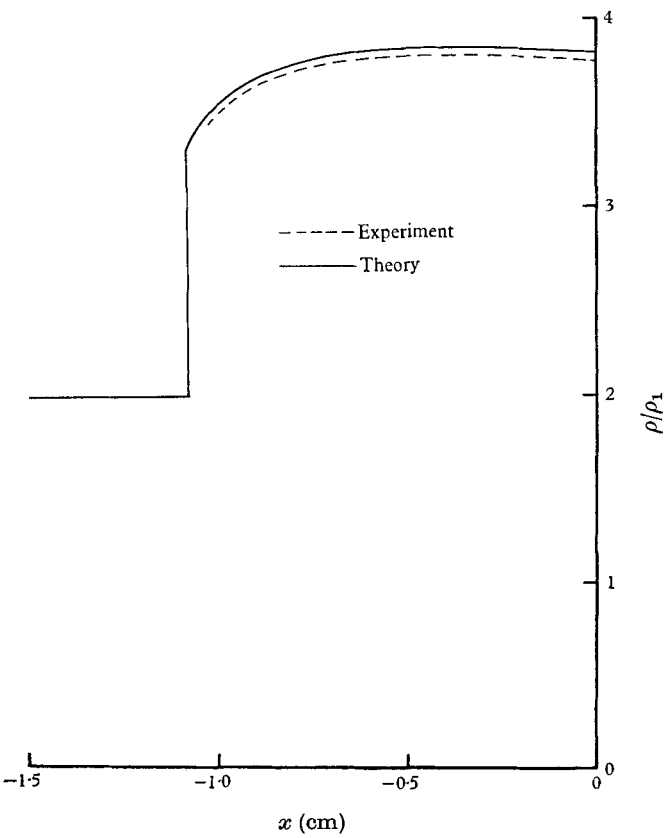

FIGURE 7. Density distribution for reflected shock wave in CO_2 with $T_1 = 295$ °K, $p_1 = 79{\cdot}6$ mmHg and $M_S = 1{\cdot}51$.

shock-wave boundary-layer interaction on the windows. Close to the end wall there is a definite departure from the theory caused by the heat transfer to the end wall which is neglected in the theory. The departure was found to increase with time, as one would expect, the cooling at the wall leading to a gradual increase in density while the pressure remains nearly constant.

Acknowledgements are made to Mr R. J. Hine for assisting with the experiments and to the Ministry of Aviation, who supported this work.

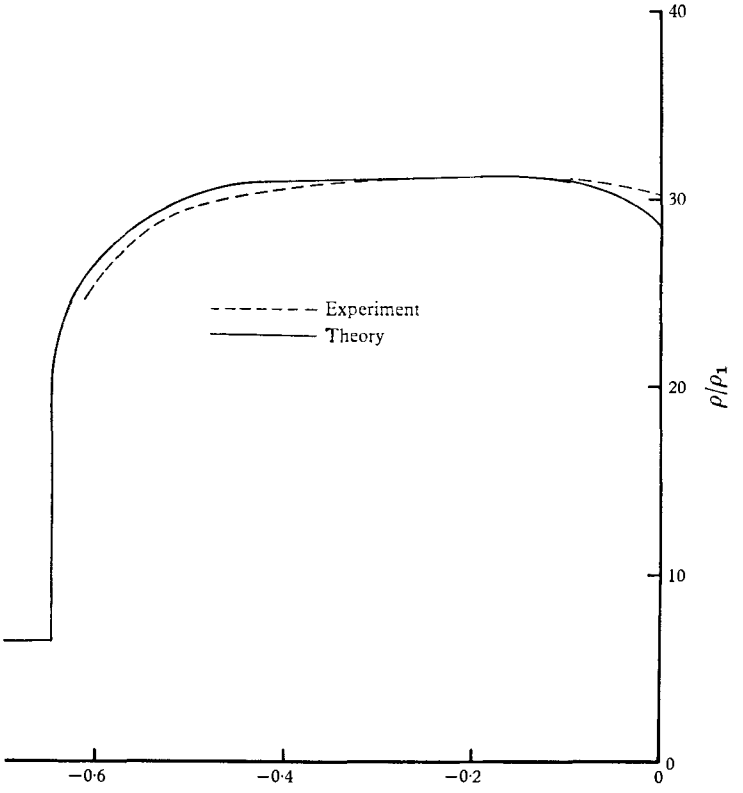

FIGURE 8. Density distribution for reflected shock wave in CO_2 with $T_1 = 295$ °K, $p_1 = 1{\cdot}53$ mmHg and $M_S = 3{\cdot}97$.

Appendix. Gradients in the flow behind the reflected shock wave

On figure A 1, A is the point of reflexion which is chosen as origin of the co-ordinate system. BCD is a particle path and DE and DF are characteristics.

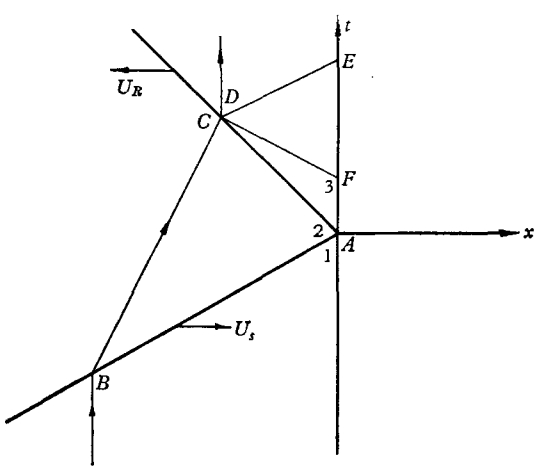

FIGURE A 1. (x, t)-diagram.

U_S is the speed of the incoming shock wave positive in the direction of the x-axis and U_R is the speed of the reflected shock wave positive in the direction opposite to x. u, v, w are particle velocities relative to the wall, to the incoming shock, and to the reflected shock, respectively. Suffixes 1, 2, 3 refer to conditions at A in the three regions shown on figure A 1. The small differences between values on the particle path and at the origin are written as differentials, e.g.

$$du_2 = u_C - u_2; \quad dp_3 = p_D - p_3. \tag{A 1}$$

From the characteristic equations (12) and (13) using $u_E = u_F = 0$ and the obvious relation $t_E + t_F = 2t_D$ it follows that

$$p_E + p_F = 2p_D. \tag{A 2}$$

This shows that, to the first order, p is independent of x in region 3. This can also be seen from the equation of motion

$$\frac{\partial u}{\partial t} + u\frac{\partial u}{\partial x} + \frac{1}{\rho}\frac{\partial p}{\partial x} = 0, \tag{A 3}$$

which shows that at the origin where $\partial u/\partial t = u = 0$ we must have $\partial p/\partial x = 0$. We can therefore write the pressure gradient at the wall as

$$(\partial p/\partial t)_{t=0} = dp_3/t_D. \tag{A 4}$$

Using standard shock-wave relations one finds

$$du_3 = \frac{w_3}{w_2}(-dv_2 + dU_R) - \frac{4}{\gamma_\alpha + 1} m_R^{-3} w_2 \left[\frac{du_2 + dU_R}{a_2} - m_R \frac{da_2}{a_2}\right] - dU_R \tag{A 5}$$

and

$$dp_3 = \frac{p_3}{p_2} dp_2 + \frac{4\gamma_\alpha}{\gamma_\alpha + 1} p_2 m_R \left[\frac{du_2 + dU_R}{a_2} - m_R \frac{da_2}{a_2}\right], \tag{A 6}$$

where

$$m_R = \frac{u_2 + U_R}{a_2}. \tag{A 7}$$

From the characteristic equations one obtains

$$dp_3 = \rho_3 a_3 du_3 \frac{t_E + t_F}{t_E - t_F} - (\gamma_\alpha - 1)\rho_3^2 \Gamma_3 t_D, \tag{A 8}$$

where

$$\Gamma = \Phi(\bar{\sigma} - \bar{\sigma}_1). \tag{A 9}$$

Eliminating du_3 and using (A 4) gives an expression for $(\partial p/\partial t)_{t=0}$ containing differentials which can be found from the Rayleigh-line equations governing the flow in region 2. These are most conveniently expressed in terms of the Mach number m_2 defined by

$$m_2 = v_2/a_2. \tag{A 10}$$

The final expression is in the non-dimensional notation

$$\left(\frac{\partial \hat{p}}{\partial \hat{t}}\right)_{\hat{t}=0} = \frac{\hat{\Phi}_2(\hat{\bar{\sigma}}_2 - \hat{\bar{\sigma}}_1)}{\hat{c}_{p\alpha} \hat{T}_1^2} G(m_2)\left[F(m_2) - \frac{\Gamma_3}{\Gamma_2}\right], \tag{A 11}$$

where $$G(m_2) = \frac{2\gamma_\alpha[(\gamma_\alpha - 1)\, m_2^2 + 2]^2}{m_2^4[2m_2^2 + (\gamma_\alpha - 1)]\,[-(\gamma_\alpha - 1)\, m_2^4 + (\gamma_\alpha + 5)\, m_2^2 + 4\gamma_\alpha - 2]}, \quad \text{(A 12)}$$

and $$F(m_2) = \frac{[m_2^2 + 1]\,[(\gamma_\alpha - 1) + 2m_2^2]\,[2\gamma_\alpha - (\gamma_\alpha - 1)\, m_2^2]\,[2 + 2\gamma_\alpha m_2^2 + (3\gamma_\alpha + 1) m_2^4 - (\gamma_\alpha - 1) m_2^6]}{2(\gamma_\alpha + 1)^3 m_2^4 (1 - m_2^2)}.$$

Figure A 2 shows $F(m_2)$ and Γ_3/Γ_2 for CO_2 (using (20) and (21)) plotted against M_S for $T_1 = 295$ °K. It follows that for CO_2

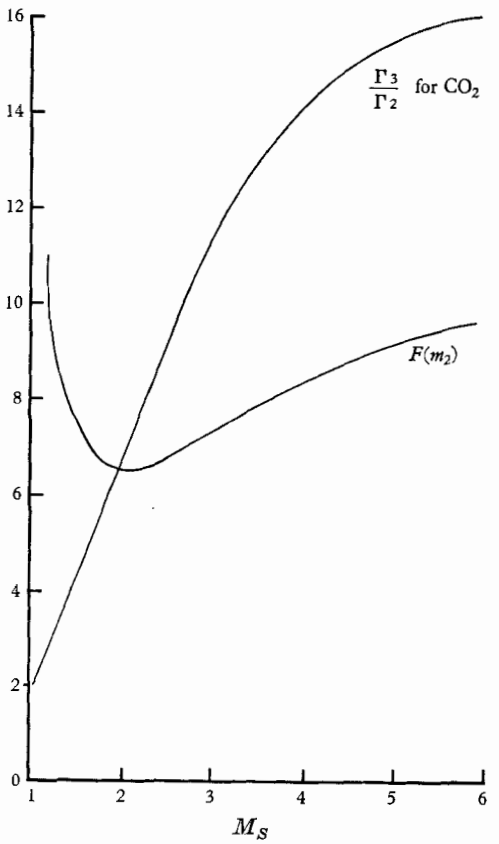

FIGURE A 2. Γ_3/Γ_2 for shock waves in CO_2 with $T_1 = 295$ °K and $F(m_2)$ as functions of M_S.

$$\left(\frac{\partial p}{\partial t}\right)_{t=0} > 0 \quad \text{for} \quad M_S < 2,$$

$$\left(\frac{\partial p}{\partial t}\right)_{t=0} < 0 \quad \text{for} \quad M_S > 2.$$

N.B. During the analysis it was found that the following simple relation holds for a reflected shock wave in an ideal gas: the Mach number of the flow in region 2 relative to the incoming shock is the reciprocal of the Mach number of the flow in region 2 relative to the reflected shock. This simple relation seems to have

escaped most writers on the subject. Von Mises (1958) relegates it to a footnote on p. 217 of his book. It is of great practical use and means that reflected shock-wave calculations can be made simply by using standard tables for normal shock waves twice.

REFERENCES

BAGANOFF, D. 1964 *Rev. Sci. Instr.* **35**, 288.

BAGANOFF, D. 1965 *J. Fluid Mech.* **23**, 209.

DYNER, H. B. 1966 *Physics of Fluids*, **9**, 879.

HILSENRATH, J. *et al.* 1955 *Nat. Bur. St. Circ.* no. 564.

HURLE, I. R., RUSSO, A. L. & HALL, J. G. 1964 *J. Chem. Phys.* **40**, 2076.

JOHANNESEN, N. H. 1961 *J. Fluid Mech.* **10**, 25.

JOHANNESEN, N. H., ZIENKIEWICZ, H. K., BLYTHE, P. A. & GERRARD, J. H. 1962 *J. Fluid Mech.* **13**, 213.

MISES, R. VON 1958 *Mathematical Theory of Compressible Fluid Flow.* New York: Academic Press.

PHINNEY, R. 1964 *A.I.A.A. J.* **2**, 240.

SHAPIRO, A. H. 1954 *The Dynamics and Thermodynamics of Compressible Fluid Flow.* New York: Ronald Press.

ZIENKIEWICZ, H. K. & JOHANNESEN, N. H. 1963 *J. Fluid Mech.* **17**, 499 (and corrigendum **18** (1964), 635).

ZIENKIEWICZ, H. K., JOHANNESEN, N. H. & GERRARD, J. H. 1963 *J. Fluid Mech.* **17**, 267.

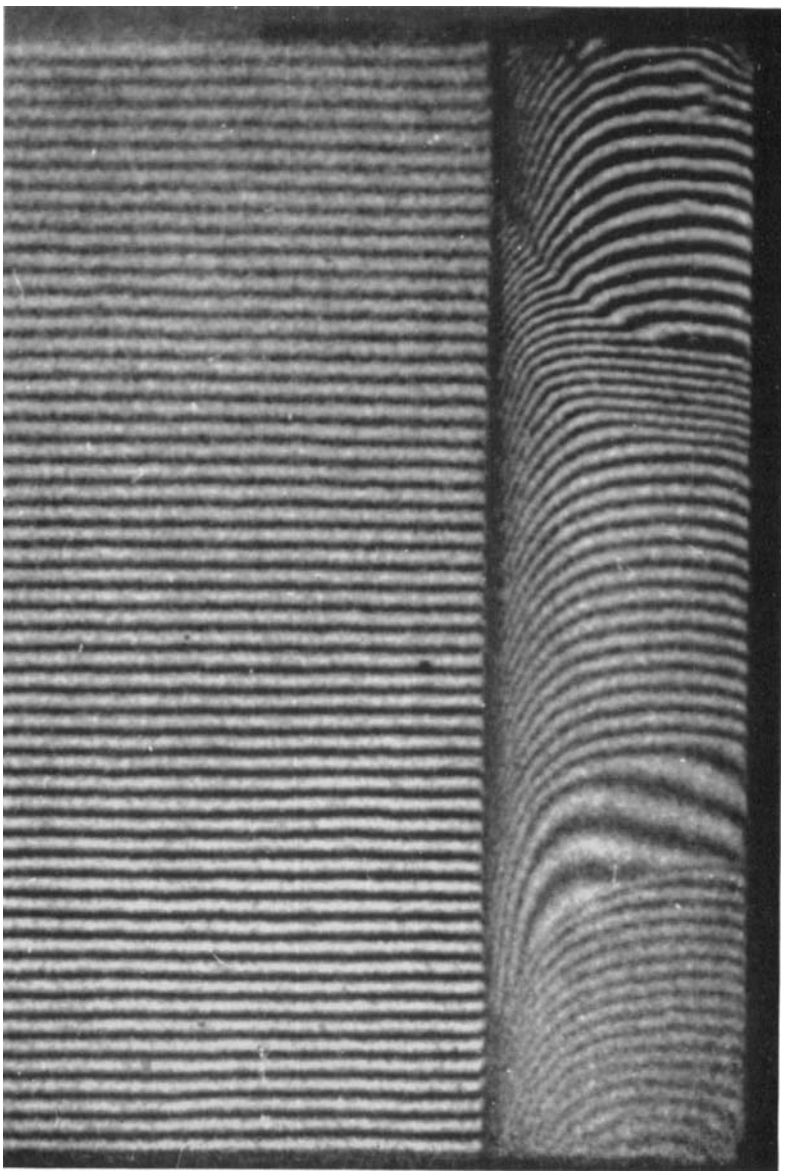

FIGURE 1. Monochromatic fringe pattern for reflected shock wave in CO_2 with $T_1 = 295$ °K, $p_1 = 79{\cdot}6$ mmHg and $M_S = 1{\cdot}50$.